

## Effects of NiMoO<sub>4</sub> impregnation on the catalytic activity of Cu<sub>3</sub>(PO<sub>4</sub>)<sub>2</sub> in the conversion of isopropanol

Mbarka OUCHABI <sup>(a)\*</sup>, Mohammed BAALALA <sup>(a)</sup>, Abdelkrim ELAISSI <sup>(a)</sup>, Ilyasse LOUILIDI <sup>(b)</sup>, Fatima BOUKHLIFI <sup>(b)</sup>, Mohammed BENSITEL <sup>(a)</sup>

<sup>(a)</sup> Laboratory of Catalysis and Corrosion of Materials, Chouaib Doukkali University, Faculty of Sciences El Jadida, BP. 20, El Jadida, Morocco

<sup>(b)</sup> Laboratory of Chemistry and Biology Applied to the Environment, Faculty of Sciences, Moulay Ismail University, BP 11,201-Zitoune, Meknes, Morocco.

### Abstract

Hereby, we are describing the synthesis and characterisation concerning acid -basic properties of catalysts containing varied amounts of NiMo (2-14 wt % of NiMoO<sub>4</sub>) worn on copper orthophosphate whose preparation was executed employing a Co-precipitation method, to which we introduced the Nickel Molybdenum by impregnation with a porous volume at several stages, succeeded by calcination under air at a different temperature. The employed techniques for solid characterisation were XRD to identify different phases, Nitrogen adsorption at -196°C. and catalytic conversion of isopropanol at different temperatures reaction ranging from 180 to 400 °C. The outcome revealed that the solids NiMo/CuP mainly consisted of copper phosphate Cu<sub>3</sub>(PO<sub>4</sub>)<sub>2</sub> together with NiMoO<sub>4</sub> as minor phase. The NiMoO<sub>4</sub> crystallinity's degree increases by increasing Nickel Molybdenum. It was discovered that the specific area (S<sub>BET</sub>) of the studied system will slightly increase by the increase in NiMoO<sub>4</sub> content. The catalytic activity in isopropanol conversion which proceeds via dehydration yielding propene increases as a function of the extent of loading.

\* Corresponding author:

[ouchabimbarka@gmail.com](mailto:ouchabimbarka@gmail.com)

Received 24 Aout 2020,

Revised 03 Mars 2020,

Accepted 05 Nov 2021

**Keywords:** Copper orthophosphate CuP; Supported Nickel Molybdenum catalysts (NiMo/CuP); XRD; BET; Isopropanol decomposition.

## 1. Introduction

For many organic processes and mainly in heterogeneous catalysts, the metal orthophosphate method has been amply used [1]. The catalytic properties of a solid depend on its structure and surface texture [2]. Such properties are acquired during its synthesis. Sometimes, some of these solids are impregnated with various compounds for different purposes. Therefore, the support's acid and basic surface properties are amended by various doping agents addition [3–6]. Recently, different magnesium orthophosphates are used as catalysts for various reactions [7–8]. Aramendia and al., have synthesised some magnesium orthophosphates and alkali magnesium orthophosphates and used them to convert the 2-Hexanol [9]. They found, in the conversion of gaseous 2-hexanol using a particular synthetic procedure, that these products show significantly variable activity and selectivity. Our group investigated the influence of the Magnesium Phosphates Catalysts Crystal Phase on the Skeletal Isomerisation of 3,3-dimethylbut-1-ene and confirmed the strong influence of the crystalline structure of magnesium phosphates [10] on the catalytic activity. In addition, the impregnation of various active species like molybdenum oxide, cobalt oxide and nickel oxide to  $\text{SiO}_2$ ,  $\text{Al}_2\text{O}_3$ , and orthophosphates alter the activity and selectivity of these catalysts in different organic processes. For example, Hailiang Yin and al. have investigated  $\text{NiMo}/\text{Al}_2\text{O}_3$  catalyst consisting of nano-sized zeolite Y for deep hydrodesulfurization and hydrodenitrogenation of diesel [11], the results proved that the catalyst including nano-sized zeolite Y bears a high level in HDS and HDN activities and shows a relative rate constantly for the removal of total sulfur or nitrogen higher than the one including micro-sized zeolite. Also Mitsugu Taniguchi demonstrated that The  $\text{Mo}_3\text{NiS}_4/\text{NaY}$  catalyst has much higher activity for HDS of benzothiophene than the  $\text{Mo}_3\text{S}_4/\text{NaY}$  catalyst [12]; Nickel impregnation into the  $\text{Mo}_3\text{S}_4$  zeolite catalysts remarkably ameliorate the HDS activity; the interaction between nickel and molybdenum in the precursor is plausible to be effective at producing active species. Aramendia and al observed the impact of  $\text{Na}_2\text{CO}_3$  impregnation on the activity of  $\text{Mg}_3(\text{PO}_4)_2$  in the dehydration 2-hexanol, and indicated the acidity of  $\text{Mg}_3(\text{PO}_4)_2$  decreases following the addition of  $\text{Na}_2\text{CO}_3$  [13]. Consequently, the conversion to N-alkylated products over  $\text{Na}_2\text{CO}_3$ -impregnated magnesium orthophosphates is clearly associated to surface acidity and hence to the carbonate content. Beside these researches, our group examined the influence of acid-base properties of cobalt-molybdenum catalysts propped on magnesium orthophosphates in isomerization of 3,3-dimethylbut-1-ene [14]. The changes in acidic properties were the main reason behind the transformations observed in catalytic activity, which depended on Co-Mo content. The isopropanol's transformation is a well-known test reaction for characterising both acidic and basic properties of solids [14–20], the particular role of each property remains uncertain. Many authors ascribe the dehydrating activity of oxides to their Bronsted surface acidity, involved in E1 mechanisms (via carbonium ions), or acid-base pairs acting through an E2 mechanism (via uncharged intermediate species). Or an E1cb mechanism (via carbanions). Furthermore, the dehydrogenation reaction seems to be concerning the catalyst's surface basicity. In a prior work [21], we have worked on reporting a synthesis related to a pure copper orthophosphate (CuP) and CuP modified by introducing vanadium (2-12 wt % of  $\text{V}_2\text{O}_5$ ) via an easy and time-saving route, compared to previous synthesis of other metal orthophosphates. At a high temperature, a thermal treatment under atmosphere leads to copper orthophosphate  $\text{Cu}_3(\text{PO}_4)_2$ , as displayed by XRD analysis, we have also demonstrated the crystallisation phase  $\text{V}_2\text{O}_5$  on the top support. In the catalytic tests concerning isopropanol transformation reaction, the highest production of propene appeared on the catalyst with the largest copper's concentration. Moreover, the existence of vanadium in the catalysts favoured new acid sites formation in the catalyst which resulted in the transformation of isopropanol to propene. Depending on the same context, in this assignment, a set of modified copper orthophosphate supports by additional Nickel Molybdenum in different content, have been synthesised by impregnation to porous

volume. The employed methods were XRD, adsorption-desorption of nitrogen and the catalytic activity of these solids was studied for the isopropanol reaction at 180-400 °C. This reaction will enable the evaluation of the acid-base properties of these catalysts.

## 2. Experimental

### 2.1. Sample preparation

Copper orthophosphate CuP was synthesised from aqueous solutions of  $\text{Cu}(\text{NO}_3)_2 \cdot 3\text{H}_2\text{O}$  and  $(\text{NH}_4)_2\text{HPO}_4$  by evaporating to dryness these latter. The following step was to dry for 12h the issued solids at 120 °C and finally to calcify it for 10h in air at 450 °C [22]. A set of nickel molybdenum (2-14%  $\text{MoO}_3$ ; 3% NiO) catalysts NiMo/CuP, was made involving successive impregnation method, over a CuP support [23]. A pile of nickel nitrate  $[\text{Ni}(\text{NO}_3)_2 \cdot 6\text{H}_2\text{O}]$  calculated to yield the desired percentage of nickel on the support, was melted in a predetermined quantity of distilled water. The calculation of this volume (Quantity) was done found on the pore volume of support. The impregnated catalysts Ni/CuP were dried for 12Hours at a temperature of 120 °C and calcined afterwards under air flow at 450 °C during 4h. A second impregnation over Ni/CuP by using an aqueous solution of ammonium heptamolybdate  $[(\text{NH}_4)_6\text{Mo}_7\text{O}_{24} \cdot 4\text{H}_2\text{O}]$ . Thereafter, the impregnated catalysts are once again dried for 12h at 120 °C and calcined under air flow at 450 °C for 4 hours, finally we calcined these solids for 10 hours at a temperature of 650 °C in order to clearly identify the phase obtained.

### 2.2. Characterization techniques

The X-ray diffraction (XRD) analysis was carried out for the fresh catalyst using Bruker-eco D8 Advance diffracts metre with Cu-K radiation ( $\lambda = 1.5418 \text{ \AA}$ ). The  $2\theta$  were scanned from 5 to 70°. Diffuse reflectance infrared spectra for the synthesised solids were recorded from 4000 to 400  $\text{cm}^{-1}$  on a Nicolet 460 spectrophotometer. The samples' textural properties (i.e. specific area, pore volume) were specified using nitrogen adsorption-desorption at -196 °C on a 3Flex Version 3.01 system.

### 2.3. Catalytic test

The process of isopropanol's decomposition was executed in a fixed-bed type reactor at an atmospheric pressure with a continuous flow system. In a glass reactor placed in a furnace, we loaded the catalyst (50 mg). However, before starting these catalytic activity measurements, we activated each catalyst sample by first being heated in a stream of nitrogen for 2 hours at 400 °C and then cooled down to reach the catalytic reaction temperature. The reactant, 2-propanol, was diluted in nitrogen by bubbling the gas through the liquid reactant in saturator maintained at 6 °C. This process was carried out at a temperature between 180 and 400 °C. The products were analysed by online gas chromatography (FID) using a 10% OV-101 on Chromosorb-WHP (80/100 mesh) packed column (4m) maintained at 80 °C. In a blank test, it has been shown an insignificant thermal reaction which was developed in the absence of the catalyst.

## 3. Results and discussion

### 3.1. XRD results

Through an interior work, using the XRD analysis, we studied the crystalline evolution of the CuP support amidst calcination [22]. Above 723 K, two crystalline materials, corresponding to  $\text{Cu}_3(\text{PO}_4)_2$  and  $\text{Cu}_2(\text{PO}_4)(\text{OH})$  phases are

clearly put in evidence. Gradually, as we increase the temperature, diffraction lines of the copper orthophosphate are sharpened and the crystalline phase  $\text{Cu}_2(\text{PO}_4)(\text{OH})$  is converted into  $\text{Cu}_3(\text{PO}_4)_2$  phase, indicating a better crystallisation of  $\text{Cu}_3(\text{PO}_4)_2$ . As shown in **figure 1**, the calcined solid CuP at 650 °C consisted of the copper orthophosphate  $\text{Cu}_3(\text{PO}_4)_2$  (PDF Index Name: Copper Phosphate ref. Cod: 01-070-0494). Solids impregnated with Nickel molybdenum were also studied. As demonstrated in **figure 1**, the calcination at 650 °C of these solids lead not only to the previous phase identified for  $\text{Cu}_3(\text{PO}_4)_2$ , but also to new diffraction lines at  $2\theta = 26^\circ$ ,  $33^\circ$  and  $38^\circ$ , has been attributed to the crystallisation phase of Nickel Molybdenum oxide  $\text{NiMoO}_4$  (ref cod: 00-045-0142), which progressively increased with the increase of Nickel molybdenum-containing load. This phase appertains to the monoclinic, spatial group C2/m (12) and is crystallised from low load over the copper phosphate's exterior. The formations of  $\text{Cu}_3(\text{PO}_4)_2$  and  $\text{NiMoO}_4$  oxide is well confirmed by XRD.

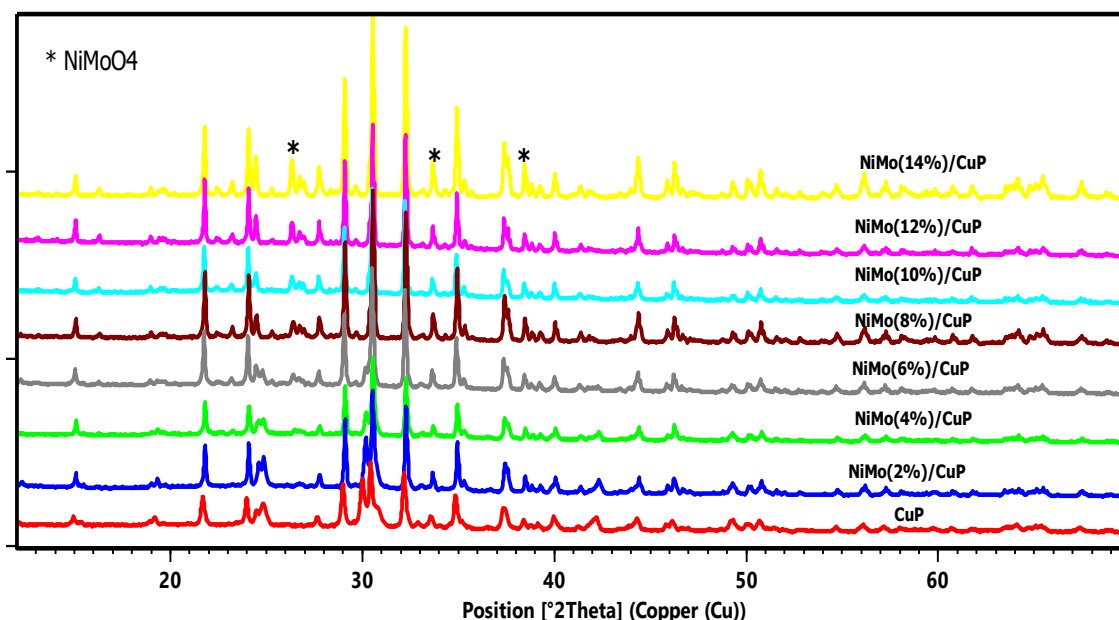


**Figure 1:** XRD Patterns of NiMo/CuP solids.

**Table 1:** Average crystallite size of NiMo/CuP solids calculated from XRD data.

Catalysts	CuP	NiMo (2%)	NiMo (4%)	NiMo (6%)	NiMo (8%)	NiMo (10%)	NiMo (12%)	NiMo (14%)
Crystallite size (nm)	40.86	40.86	40.86	40.86	40.86	40.86	40.86	40.86

However, Average NiMo/CuP crystallite size calcined at 650 °C was calculated by applying the Debye-scherrer's equation from the top score software and reported in **table 1**. The compositions of these solids are Nanocrystalline with 40nm as an average crystallite size. The crystallite size of all solids calcined at 650 °C remains stable which confirms the better catalysts crystallisation.

### 3.2. FTIR results

The FTIR spectra related to synthesised NiMo/CuP is viewed on **figure 2**. For characteristic vibration of CuP calcined at 650 °C, FTIR bands are affected by the literature [24, 25] based on the fundamental vibrating unit  $\text{PO}_4^{3-}$  anion. The existence of the strong bands at 1120, 965-935, 608-527 and  $406\text{ cm}^{-1}$  is considered one of the most noteworthy spectrum's features. These bands can be attributed to the  $\nu_{\text{as}}(\text{PO}_4^{3-})$ ,  $\nu_{\text{s}}(\text{PO}_4^{3-})$ ,  $\delta_{\text{s}}(\text{PO}_4^{3-})$  and  $\delta_{\text{s}}(\text{POP})$ , respectively. The characteristic bands of groups ( $\text{PO}_4^{3-}$ ) refine, and divide, which reflects a structural development of crystalline compound. For FTIR spectra of NiMo/CuP (**figure 2**) and compared to the CuP samples, and the appearance of the bands at 738, 820 and  $870\text{ cm}^{-1}$  indicates the presence of weakly crystallised  $\text{NiMoO}_4$ . From literature, the spectrum of molybdate is distinguished by the appearance of three strong absorption bands at 566, 762 and  $848\text{ cm}^{-1}$ . The first two are assigned to Mo-O stretching vibrations with Mo in octahedral coordination. The band at  $848\text{ cm}^{-1}$  indicates that part of the Mo is in a tetrahedral environment[26]. In this case, the broad band centred around  $738\text{ cm}^{-1}$  assigned to Mo-O stretching vibrations with Mo in octahedral coordination. The band at  $467\text{ cm}^{-1}$  (due to Mo-O octahedral vibration) is absent, perhaps they could have been masked by the band's characteristic of phosphates.

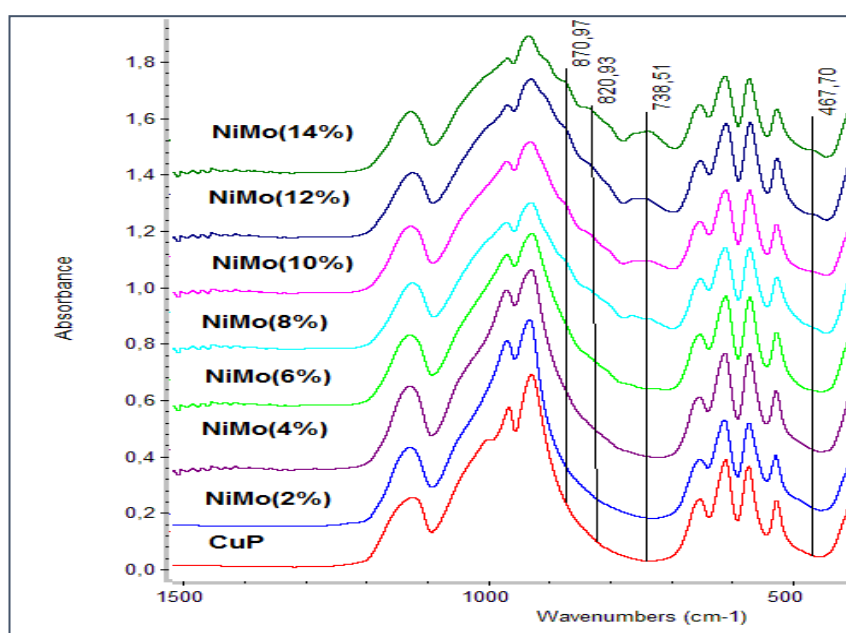


**Figure 2.** FTIR spectra of NiMo/CuP solids.

Initial conditions: All solids are calcined at 650 °C, Region from 1500 to  $400\text{ cm}^{-1}$ .

### 3.3. Textural properties of the calcined solids

The nitrogen adsorption-desorption isotherms of the CuP support and those of representative NiMo/CuP obtained by impregnation method are reported in the **figure 3**. All the solids have an adsorption-desorption isotherm as intermediate between type II and IV corresponding to non-porous or macro porous materials. At low relative pressure formation of a monolayer of adsorbed molecules is the prevailing process, while at high relative pressure a multiplayer adsorption takes place: the adsorbate thickness progressively increases until condensation pressure has been reached, the pressure of the first monolayer formation is lower if the interaction between adsorbate and adsorbent is stronger, but monolayer formation processes are always overlapped[27]. The isotherms of the CuP show parallel adsorption and desorption branches and a well-defined hysteresis loop in the relative pressure range  $p/p^0 = 0.2-1$ . It corresponds to the

type as intermediate between type H3 and H4 according to the IUPAC classification (International Union of Pure and Applied Chemistry). These hysteresis (type H3) is usually found on solids consisting of aggregates or agglomerates of particles forming slit shaped pores (plates or edged particles like cubes), with uniform (type H4) or nonuniform (type H3) size and/or shape. The hysteresis is usually due to a different behaviour in adsorption and desorption. For example, in pore formed by parallel plates the meniscus is flat (radius =  $\infty$ ) during adsorption (condensation does not take place at any relative pressure) and cylindrical (radius = half the distance between plates) during desorption.

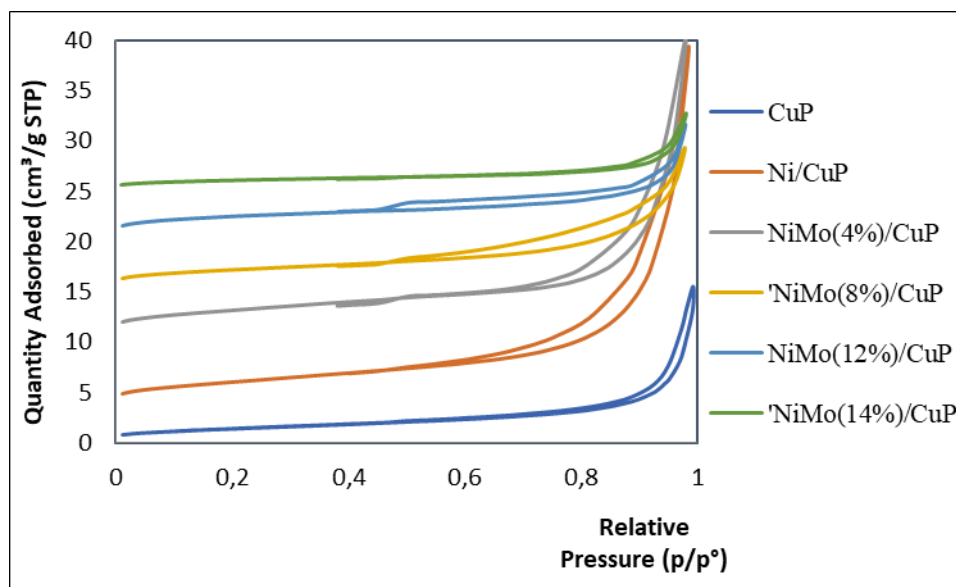


**Figure 3:** Nitrogen adsorption-desorption isotherms of raw CuP and NiMo/CuP catalysts.

Initial conditions: All catalysts are calcined at 450 °C; Column flow rate: 2cc/min; Saturation pressure: 28mmHg ;H<sub>2</sub> flow rate: 25cc/min; Nitrogen flow through the Colum: 5cc/min. (For a better visibility, the isotherms are shifted along the Y-axis).

A summary of the different surface parameters of these solids, namely specific surface area ( $S_{BET}$ ), total pore volume ( $V_p$ ) and average pore diameter ( $d_p$ ), is defined in Table 2. The majority of them have a low surface area that increases by increasing NiMoO<sub>4</sub> content when comparing it to the CuP. It's noteworthy that NiMo/CuP samples exhibit slightly higher specific BET surface areas (11.02 m<sup>2</sup>/g) and pore volume (0.033 cm<sup>3</sup>/g) in comparison to those CuP pure (6.1 m<sup>2</sup>/g; 0.017 cm<sup>3</sup>/g). The remarked increase in the  $S_{BET}$  and pore volume of NiMo/CuP system is caused by the NiMoO<sub>4</sub> oxide doping carried out at 450 °C which could be assigned to the formation of new pores during the thermal treatment of the doped impregnated solids through the liberation of nitrogen oxide gases during thermal decomposition of nickel nitrate when dopant was added. Similar results were reported in the situation of CuO-ZnO/Al<sub>2</sub>O<sub>3</sub>[28], Cr<sub>2</sub>O<sub>3</sub>/Al<sub>2</sub>O<sub>3</sub>[29] and NiO/Al<sub>2</sub>O<sub>3</sub> systems[30]. The observed transformations in the surface characteristics of the system in question since there is a high possibility to get changes in its catalytic activity as an aftermath due to doping with NiMoO<sub>4</sub>. In the case of NiMo/CuP (14%) there is a decrease in the specific surface area and the pore volume, which can result in the coverage of the surface by NiMoO<sub>4</sub> species which goes along with the result of XRD analysis. This effect has been observed in the deposition of alkali metals on oxide supports [31].

The alkali metal-impregnated support has a lower specific surface area, whatever the calcination temperature is. This may be affected to a 'cement effect' that glues the support and alkali metal salt with each other in a sort of conglomerate [31]. Although the average pore diameter for these solids is in the mesoporous range, as a matter of fact,



most of pores are macropores. As a result, both the specific surface area and the cumulative volume pore are rather small, relative to other phosphate catalysts [8].

**Table .2:** Specific surface area ( $S_{BET}$ ), cumulative pore volume ( $V_p$ ), and average pore diameter ( $dp$ ), for the catalysts NiMo/CuP. Initial conditions: All catalysts are calcined at 450 °C.

Catalysts	$S_{BET}$ (m <sup>2</sup> /g)	$V_p$ (cm <sup>3</sup> /g)	$dp$ (nm)
CuP	6.1	0.017	11
Ni	10.78	0.031	14.2
NiMo (4%)	11.02	0.033	15.7
NiMo (8%)	7.58	0.0163	10.8
NiMo (12%)	8.85	0.011	8.12
NiMo (14%)	4.01	0.0078	12.07

### 3.4. Catalytic activities of various catalysts

The isopropanol's transformation is frequently used as a test reaction to define acid base properties of oxide catalysts[32]. The reaction can give as main products acetone, propene and, to a lesser extent, diisopropyl ether. Dehydration at acid sites or concerted acid base pair sites produce propene and diisopropyl ether, and dehydrogenation at basic sites produce acetone. Ether formation must involve an intermolecular coupling reaction. The isopropanol dehydration's mechanism has been interpreted many times and many of them are contradictory, also isopropanol transformation cannot be used as a simple test of acidity[31] . Besides, the isopropanol decomposition reaction cannot distinguish between the Lewis and Bronsted sites. The existence of species with redox properties, like the nickel molybdenum in the catalysts synthesised in this study, can be very crucial in the isopropanol dehydration and dehydrogenation reactions. The catalytic transformation of isopropanol was conducted over NiMo/CuP solids containing different amounts of Nickel Molybdenum and exposed to a heat treatment at 450 °C. The catalytic reaction was executed at temperatures between 180 °C and 400 °C. The catalytic reaction product was propene only for all investigated catalyst samples, which acted only as dehydration catalysts (**Table 3**). The presence of nickel molybdenum on the oxides favoured the formation of acid sites (Lewis and Bronsted) that would participate in the creation of the propene in all the samples. Therefore, it is essential to emphasise that the lack of information about the interaction of nickel molybdenum in the structure of the CuP prevented a better interpretation of the obtained results in this study. All values shown were gathered at  $t = 140$  min, which confirms that the activity remained constant over time at 240 °C **figure 4**, **figure 5** and **figure 6** show that the conversion of isopropanol was variable depending on the reaction temperature and of the Nickel Molybdenum content respectively, for the catalytic reaction conducted over NiMo/CuP solids pre-calcined at 450 °C. Inspection of **figure 5** and **figure 6** revealed that: (i) The isopropanol conversion's rate increased progressively depending on the reaction temperature. (ii) The catalytic activity vis-à-vis the increase of isopropanol conversion by the increase in the NiMoO<sub>4</sub> content. In preliminary experiments, the CuP support material preheated at 450 °C showed extremely small catalytic activity against isopropanol conversion. So, in this study case, NiMoO<sub>4</sub> can be considered as the pro-active constituent. The detected rise in the catalytic activity of the studied samples over the increase of NiMoO<sub>4</sub> content can result in a continuous increase in the active sites 'concentration participating in the catalytic dehydration process of isopropanol. The observed decline in the catalytic

activity for NiMo (14%)/CuP could be discussed regarding a possible declining in concentration of surface OH-groups, which participate in the catalytic reaction [34] and to a possible effective dissolution of NiMoO<sub>4</sub> in CuP lattice forming NiMo/CuP solid solutions as well, which exhibited a catalytic activity small. Also, could be caused by blockage of some surface active sites by NiMo not directly taking part in the dehydration process of isopropanol [31].

**Table 3:** Isopropanol conversion (%) and selectivity towards propene, acetone Over NiMo/CuP catalysts. Initial conditions: The masse of the catalyst is 50 mg, all catalysts are calcined at 450 °C. The isopropanol decomposition was performed at a temperature 240 °C.

Catalysts	specific (m <sup>2</sup> /g)	area	Conversion (%)	S <sub>propene</sub> (%)	S <sub>acetone</sub> (%)	Catalyticactivity	
						mmol/h/g	mmol/h/m <sup>2</sup>
<b>CuP</b>	6.1		20	100	0	2.50E-06	4.10E-07
<b>Ni/CuP</b>	10.78		30	99	1	3.75E-06	3.48E-07
<b>NiMo (2%)/CuP</b>	-		45	99	1	5.63E-06	-
<b>NiMo(4%)/CuP</b>	11.02		55	97	3	6.88E-06	6.24E-07
<b>NiMo(6%)/CuP</b>	-		56	97	3	7.00E-06	-
<b>NiMo (8%)/CuP</b>	7.58		58	96	4	7.25E-06	9.56E-07
<b>NiMo (10%)/CuP</b>	-		62	96	4	7.75E-06	-
<b>NiMo (12%)/CuP</b>	8.85		70	97	3	8.75E-06	9.89E-07
<b>NiMo (14%)/CuP</b>	4.01		50	97	3	6.25E-06	15.6E-07

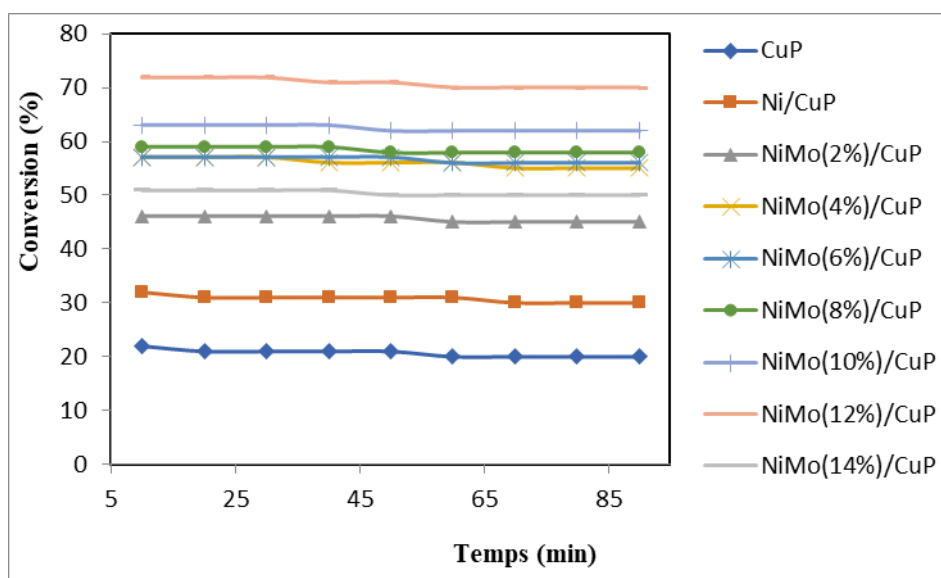


**Figure 4:** Isopropanol decomposition as function of the time reaction on NiMo/CuP catalysts. Initial conditions: The masse of the catalyst is 50 mg, all catalysts are calcined at 450 °C. The isopropanol decomposition was performed at a temperature 240 °C.



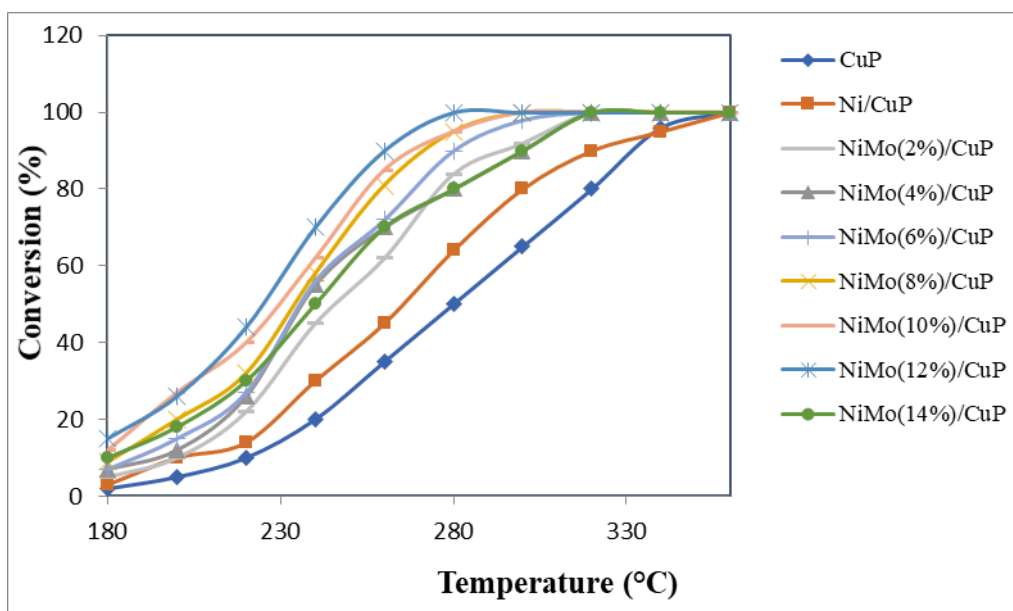


**Figure 5:** Isopropanol decomposition as function of the reaction temperature on NiMo/CuP catalysts. Initial conditions: The masse of the catalyst is 50 mg, all catalysts are calcined at 450 °C. The isopropanol decomposition was performed at a temperature between 180 and 380 °C.

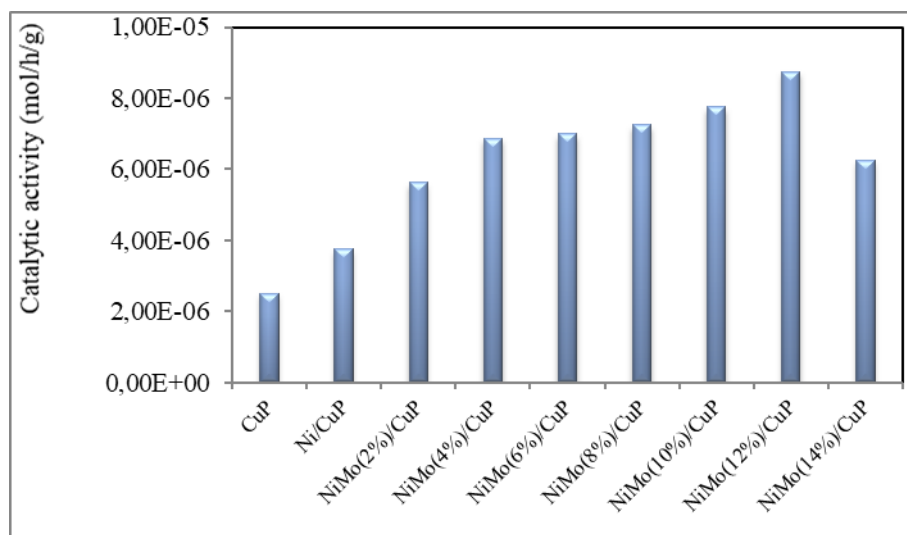


**Figure 6:** Catalytic activity of NiMo/CuP catalysts in decomposition of isopropanol. Initial conditions: The masses of the catalyst is 50 mg, all catalysts are calcined at 450 °C. The isopropanol decomposition was performed at a temperature 240 °C.

The energy's activation determined by the Arrhenius plots for isopropanol conversion is too given between 180 and 220 °C. Obviously, the highest activation energy was achieved on CuP, while it decreased when nickel molybdenum oxide content increased. We can presume that the properties of the surface are highly related to nickel molybdenum oxide load. For example, the highest content of NiMoO<sub>4</sub> phase makes easier the accumulation of coke on the surface

catalysts. The apparent activation energy ( $E_a$ ) for the catalytic conversion of isopropanol can be figured out by yielding propene in the existence of pure and doped NiMo/CuP system which enlightened us to a possible change in the mechanism of the catalysed reaction. Thus, the obtained values of  $k$  at different reaction temperatures ranged from 180 to 220 °C and over the variously treated solids have allowed to get the ( $E_a$ ) via the direct application of Arrhenius equation:  $K(t) = A e^{-E_a/RT}$ . The valours of ( $E_a$ ) thus obtained are shown in **figure 7**. An examination of the **figure 7**, revealed that: (i) By augmenting the extent of NiMoO<sub>4</sub> loading adduced a decline in the value of  $E_a$ . Simultaneously to the flow of these results, we remarked a continuous rising in the catalytic activities of the investigated solids as a result of increasing the extent of loading. The impregnating process didn't change the activation energy of the catalysed reaction but rather modified the concentration of the catalytic active constituents without modifying their energetic nature. In other words, NiMo/CuP did not modify the mechanism of catalytic conversion of isopropanol but alters the concentration of catalytically active constituents.

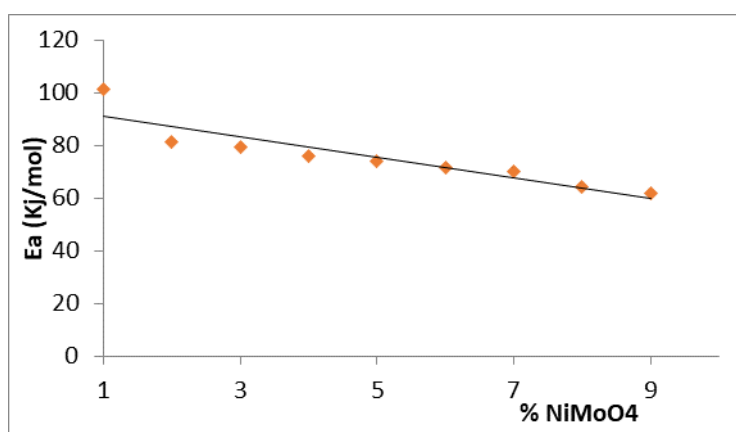


**Figure 7:** Activation energy as function of the Nickel Molybdenum oxide content for various NiMo/CuP catalysts. Initial conditions: The mass of the catalyst is 50 mg, all catalysts are calcined at 450 °C. The isopropanol decomposition was performed at a temperature between 180 and 200 °C.

## 4. Conclusion

Hereby, we have addressed the synthesis of a pure copper orthophosphate (CuP) and CuP modified by injecting the nickel molybdenum via an easy way, setting side by side with the previous synthesis of other metal orthophosphates. The generation of Cu<sub>3</sub>(PO<sub>4</sub>)<sub>2</sub> products was proved by the XRD results and the accumulation of the NiMoO<sub>4</sub> on the surface of support was also demonstrated. According to the isopropanol transformation reaction's catalytic tests, it was concluded that the catalyst with the largest concentration of copper produced the highest amount of propene. Moreover, the existence of Nickel Molybdenum in the catalysts favoured the production of new acid sites in the catalyst, which is the reason behind the conversion of isopropanol to propene. It was confirmed as well that the NiMo (12%)/CuP sample exhibited high catalytic activity in the isopropanol decomposition than other samples. The isopropanol dehydration to propene is the predominant reaction and proceeds through an elimination E1-like mechanism catalysed by acid sites. In perspective, these catalysts NiMo/CuP will be adopted in hydrodesulfuration reaction.

## References

- [1] Moffat JB. *Rev Chem Intermed*, 8 (1987)1–20.
- [2] J.M. Campelo, A. Garcia, J.M. Gutierrez, D. Luna, J.M. Marinas, *Journal of Colloid and Interface Science*, 95 (1983) 544-550.
- [3] Campelo JM, Garcia A, Gutierrez JM, *Can J Chem*, 62 (1984) 1455–1458.
- [4] D. Aman, D. R. A. El-Hafiz, and M. A. Ebiad, “Thermodynamic parameter for steam reforming reaction of biodiesel by-product using nano-sized perovskite catalysts,” *Moroccan J. Chem.*, vol. 6, no. 3, pp. 466–479, 2018.
- [5] I. R. Parrey and A. A. Hashmi, “Catalytic Hydroxylation of Phenols using Schiff base complex of Copper metal complexes derived from L-histidine,” *Moroccan J. Chem.*, vol. 3, no. 1, pp. 147–151, 2015.
- [6] Lin CH, Campbell KD, Wang JX, Lunsford JH, *J Phys Chem*. 90 (1986) 534–537.
- [7] María Angeles Aramendía, Victoriano Borau, César Jiménez, José María Marinas, Francisco José Romero, *Journal of Colloid and Interface Science* 219 (1999) 201-209.
- [8] María Angeles Aramendía, Victoriano Borau, César Jiménez, José María Marinas, Francisco José Romero, *Journal of Colloid and Interface Science*. 217 (1999) 288-298.
- [9] M. Sadiq, M. Abdennouri, N. Barka, M. Baalala, C. Lamonier, M. Bensitel, *Canadian Chemical Transactions*. 3 (2015) 225-233.
- [10] Hailiang Yin, Tongna Zhou, Yunqi Liu, Yongming Chai, Chenguang Liu, *Journal of Natural Gas Chemistry*. 20 (2011) 441–448.
- [11] Murata T, Mizobe Y, Gao H, *J Am Chem Soc*. 116 (1994) 3389–3398.
- [12] Petitjean H; Guesmi H; Lauron-Pernot H., *ACS Catal*. 4 (2014) 4004–4014.
- [13] M. Sadiq; A. Sahibed-dine; M. Baalala; K. Nohair; M. Abdennouri; M. Bensitel; C. Lamonier; J. Leglise, *Arabian Journal of Chemistry*. 4 (2011) 449–457.
- [14] Lopez-Pedrajas S; Estevez R; Blanco-Bonilla F, *J Chem Technol Biotechnol*. 92 (2017) 2661–2672.
- [15] D. Kulkarni; I.E. Wachs. *Appl. Catal. A: Gen*. 237 (2011) 121–137.
- [16] Chen X; Shen YF; Suib SL; O’Young CL, *Chem Mater*. 14 (2002) 940–948.
- [17] H.G. El-Shobaky; A.S. Ahmed; N.R.E. Radwan. *J. Colloid Surf. A: Physicochem. Eng. Aspects*. 274 (2006) 138–144.
- [18] E. Ortiz-Islasa, T. Lopez, J. Navarrete, X. Bokhimi, R. Gomez, *J. Mol. Catal. A: Chem*. 228 (2005) 345–350.
- [19] M. Sadiq; M. Bensitel; K. Nohair; J. Leglise; C. Lamonier., *J. Saudi Chem. Society*. 2012.16, 445–449.
- [20] M. Ouchabi; M. Baalala; A. Elaissi; M. Sadiq; M. Bensitel, *IOSR Journal of Applied Chemistry*. 9 (2016) 45-51.
- [21] M. Ouchabi; M. Baalala; A. Elaissi; M. Bensitel., *J. Mater. Environ. Sci*. 7 (2016) 1417–1424.
- [22] Ouchabi M; Baalala M; Elaissi A , *IOP Conference Series: Materials Science and Engineering*. Institute of Physics Publishing. 186 (2017) 12-13.
- [23] G. Leofanti; M. Padovan; B. Tozzola; B. Venturelli., *Catal. Today*. 41 (1998) 207–219.
- [24] H.G. El-Shobaky; G.M. Mohamed; G.A. El-Shobaky, *Appl. Catal. A: Gen*. 180 (1999) 335–344.
- [25] H.G. El-Shobaky; A.M. Ghozza; G.A. El-Shobaky; G.M. Mohamed, *Colloids and Surf. A: Physicochem. Eng. Aspects*. 152 (1999) 315–326.
- [26] A.S. Ahmad; G.A. El-Shobaky; A.N. Al-Noaimi; H.G. El-Shobaky., *Mater. Lett*. 26 (1996) 107–112.
- [27] V. Perricho; M.C. Durupty, *Appl. Catal*. 42 (1988) 217-227.

- [28] V.K. Díez;C.R. Apestegía;J.I. Di Cosimo., J. Catal. 215 ( 2003) 220–233.
- [29] D. Haffad; A. Chambellan; J.C. Lavalley., J. Mol. Catal. A: Chem. 168 (2001) 153–164.
- [30] S.A. El-Molla;M.N. Hammed;G.A. El-Shobaky., Mater. Lett. 58 (2004) 1003–1011.
- [31] De Zani D; Colombo M., J Flow Chem. 2 (2012) 5–7.